Transcriptomics and proteomics show that selenium affects inflammation, ctoskeleton, and cancer pathways in human rectal biopsies

The FASEB Journal article fj.201600251R. Published online May 2, 2016.

THE FASEB JOURNAL • RESEARCH • www.fasebj.org

Transcriptomics and proteomics show that selenium affects inflammation, cytoskeleton, and cancer pathways in human rectal biopsies

Catherine Méplan,[*,†,‡,§,1] Ian T. Johnson,[¶] Abigael C. J. Polley,[¶] Simon Cockell,[‖] David M. Bradburn,[#] Daniel M. Commane,[‡] Ramesh P. Arasaradnam,[†,#,] Francis Mulholland,[¶] Anze Zupanic,[*] John C. Mathers,[‡,**] and John Hesketh[*,‡,§]**

[*]Institute for Cell and Molecular Biosciences, [†]School of Biomedical Sciences, [‡]Human Nutrition Research Centre, [§]The Medical School, [‖]Bioinformatics Support Unit, and [**]Institute of Cellular Medicine, Newcastle University, Newcastle-upon-Tyne, United Kingdom; [¶]Institute of Food Research, Norwich Research Park, Norwich, United Kingdom; and [#]Wansbeck General Hospital, Ashington, United Kingdom

ABSTRACT: Epidemiologic studies highlight the potential role of dietary selenium (Se) in colorectal cancer prevention. Our goal was to elucidate whether expression of factors crucial for colorectal homoeostasis is affected by physiologic differences in Se status. Using transcriptomics and proteomics followed by pathway analysis, we identified pathways affected by Se status in rectal biopsies from 22 healthy adults, including 11 controls with optimal status (mean plasma Se = 1.43 μM) and 11 subjects with suboptimal status (mean plasma Se = 0.86 μM). We observed that 254 genes and 26 proteins implicated in cancer (80%), immune function and inflammatory response (40%), cell growth and proliferation (70%), cellular movement, and cell death (50%) were differentially expressed between the 2 groups. Expression of 69 genes, including selenoproteins W1 and K, which are genes involved in cytoskeleton remodelling and transcription factor NFκB signaling, correlated significantly with Se status. Integrating proteomics and transcriptomics datasets revealed reduced inflammatory and immune responses and cytoskeleton remodelling in the suboptimal Se status group. This is the first study combining omics technologies to describe the impact of differences in Se status on colorectal expression patterns, revealing that suboptimal Se status could alter inflammatory signaling and cytoskeleton in human rectal mucosa and so influence cancer risk.—Méplan, C., Johnson, I. T., Polley, A. C. J., Cockell, S., Bradburn, D. M., Commane, D. M., Arasaradnam, R. P., Mulholland, F., Zupanic, A., Mathers, J. C., Hesketh, J. Transcriptomics and proteomics show that selenium affects inflammation, cytoskeleton, and cancer pathways in human rectal biopsies. FASEB J. 30, 000–000 (2016). www.fasebj.org

KEY WORDS: selenoprotein · NFκB · colorectal · cytokeratin · nutrigenomics

Low intake of the dietary antioxidant micronutrient selenium (Se) is associated with increased risk of colorectal adenoma and of colorectal cancer (CRC) mortality (1); for example, in the double-blind, randomized, placebo-controlled Nutrition Prevention Cancer Trial, there was a significant (58%) reduction in CRC incidence in people receiving 200 μg supplementary Se in the form of Se-enriched yeast/d (2), and the strongest effect of Se supplementation was observed in subjects within the lowest tertile for plasma Se at the start of the trial (<1.34 μM). In contrast, in the Women's Health Initiative and Selenium and Vitamin E Cancer Prevention Trial (SELECT) trials, no benefit of increased Se intake was observed for individuals with high Se intakes (3, 4). Recent data from a European Prospective Investigation into Cancer and Nutrition (EPIC) cohort revealed that, in most European countries, plasma Se status is suboptimal and is associated with increased risk of CRC in women (5). Moreover, evidence from animal models showed that Se supplementation can prevent chemically induced colorectal carcinogenesis (6, 7). Taken together, these data support a role for Se in reducing risk of CRC initiation and progression;

ABBREVIATIONS: 2-D gel, 2-dimensional polyacrylamide gel electrophoresis; AQPs, aquaporines; CRC, colorectal cancer; EPIC, European Prospective Investigation into Cancer and Nutrition; FC, fold change; GPX, glutathione peroxidase; IEF, isoelectric focusing; IPA, Ingenuity Pathway Analysis; MALDI/ToF, matrix-assisted laser desorption ionization time-of-flight; MS, mass spectrometry; Se, selenium; SELK, selenoprotein K; SEPP, selenoprotein P; SEPW, selenoprotein W

[1] Correspondence: Newcastle University, The Medical School, School of Biomedical Sciences, Framlington Place, Newcastle-upon-Tyne, NE2 4HH, United Kingdom. E-mail: catherine.meplan@ncl.ac.uk

doi: 10.1096/fj.201600251R
This article includes supplemental data. Please visit *http://www.fasebj.org* to obtain this information.

however, the intake at which Se has cancer-preventive properties and the mechanisms underlying its anticarcinogenic properties remain unclear.

The biologic actions of Se are thought to be mediated largely by selenoproteins in which Se is incorporated in the form of the amino acid selenocysteine. Functional genetic polymorphisms in selenoprotein genes (*GPX4*, *SEPP1*, *SELS*, and *GPX1*) modulate risk of CRC or inflammatory responses (8, 9), in combination with Se status (9). Selenoproteins are crucial in the biochemical pathways essential for colorectal function, including redox control and responses to inflammatory, oxidative, and endoplasmic reticulum stress (10). For example, GPx4 expression was necessary for mitochondrial function and NFκB response to TNFα in a human colorectal adenoma cell model (11, 12), and Se intake affected mRNA mTOR, TNFα, and NF-κB signaling pathways in the colon of mice fed a marginally Se-deficient diet (13). Thus, the protective effect of Se appears to be mediated through the role of selenoproteins in molecular pathways that help to maintain homeostasis when cells experience oxidative and inflammatory challenges (9). However, the effects of Se status on such pathways within the human colorectal epithelium remain poorly understood.

To identify key factors and pathways affected by Se status, we combined transcriptomics and proteomics in a comprehensive, unbiased analysis of rectal biopsy specimens from healthy participants. For the first time, we have shown in humans that differences in Se status within the physiologic range affect global gene expression patterns in the human rectum. We found that Se status affected factors implicated in inflammatory signaling, immune function, and cytoskeleton remodelling. These findings provide insights into the mechanisms through which Se may influence cancer risk and may help in the development of early biomarkers of disease risk.

MATERIALS AND METHODS

Study population and sample collection

A subgroup of 22 adults who took part in the Biomarkers of Risk of Colorectal Cancer (BORICC) study were recruited from patients attending for routine flexible sigmoidoscopy at Wansbeck General Hospital (14), but shown to be free of colorectal disease. Ethics approval was granted by the Northumberland Local Research Ethics Committee, and research governance was obtained from the Northumberland Healthcare Trust (NLREC2/2001). Exclusion criteria included the presence or history of colonic inflammation, colorectal cancers or polyps, or a strong family history of colorectal cancer. Biopsies were performed in individuals who had no evidence of colorectal neoplasia or inflammatory bowel disease at endoscopy. Mucosal pinch biopsies were obtained from anatomically normal mucosa 10 cm from the rectal verge, snap frozen in liquid nitrogen for proteomic analysis or placed immediately in RNAlater (Thermo Fisher Scientific Life Sciences, Paisley, United Kingdom) for transcriptomic analyses, and stored at −80°C. Plasma Se concentration was measured by inductively coupled plasma mass spectrometry (MS).

RNA isolation and microarray analysis

RNA extraction was performed with Trizol (Thermo Fisher Scientific Life Sciences), according to standard procedures. Briefly, RNAlater was drained from the biopsy specimens before they were submerged in 0.5 ml Trizol. After homogenizing the tissues on ice, an additional 0.5 ml Trizol was added, and samples were incubated for 5 min at room temperature. Samples were centrifuged (10 min, 12,000 *g*, 4°C), supernatants were extracted for 3 min with 0.2 ml chloroform per 0.2 ml Trizol) and centrifuged (15 min, 12,000 *g*, 4°C), and the upper phase was precipitated in 70% EtOH prepared in diethylpyrocarbonate-treated milliQ water (EMD–Millipore, Billerica, MA, USA). Samples were purified on a PureLink RNA cartridge (Thermo Fisher Scientific Life Sciences) and eluted in RNase-DNase–free water. RNA integrity was determined by capillary electrophoresis with a Bioanalyzer Nano chip (Agilent Technologies, Stockport, United Kingdom) before microarray analysis, using whole-genome HumanHT-12, v3 single-color bead chips (Illumina, San Diego, CA, USA). Microarray results were confirmed by real-time PCR; however, because the biopsy specimens were very small, the amount of RNA was sufficient to confirm only the expression of 2 genes and a housekeeping control used to normalize the data.

Protein preparation and gel electrophoresis

Proteins were extracted from thawed tissue with a modified ReadyPrep Sequential Extraction Kit (Bio-Rad, Hemel Hempstead, United Kingdom), and the specimens were homogenized with a hand-operated micropestle (Eppendorf, Hamburg, Germany) before sonication in an ice-water bath for 10 min. The samples were centrifuged, and aliquots of supernatants were stored at −80°C. Proteins were separated by 2-D electrophoresis (15). Separation of proteins in the first dimension was performed by isoelectric focusing (IEF), with 24 cm immobilized pH gradient strips (pH 4–7) run on an Ettan IPGphor bed (GE Healthcare, Pittsburgh, PA, USA) with a step-n-hold protocol of 500 V for 0.5 kVh; a gradient of 1000 V for 0.8 kVh; a gradient of 8000 V for 13.5 kVh; and a step-n-hold of 8000 V for 30.0 kVh at 20°C, giving a total of 44.8 kVh (8 h 49 min) with a rate-limiting factor of 50 μA. After completion of IEF, the strips were stored at −80°C. The 2-dimension protein separation was carried out on 1 mm thick 10% Duracryl homogenous gels [30% acrylamide with 0.65% *N*,*N*-methylene bis-acrylamide cross-linker, 1.5 M Tris (pH 8.7–9.0), 3.6 mM SDS, 0.5 ml/L tetramethylethylenediamine, and 11 mM ammonium persulfate, prepared in-house in 28 × 23 cm gel-plate cassettes]. Electrophoresis conditions were set to give an top voltage of 500 V, power of 20 W/gel, and a total run time of ~4.5 h. Gels were stained with SYPRO Ruby fluorescent stain (Bio-Rad) and imaged with a Pharos FX Plus molecular imager (Bio-Rad; 532 nm excitation laser and 605 nm emission filter at 100 μm resolution). Using Progenesis SameSpot software (Nonlinear Dynamics, Newcastle, United Kingdom), an experienced operator aligned the gel images to a single reference image, chosen for its overall quality and spot clarity, and protein spots were quantified. At this stage, staining artifacts were removed manually, and undetected double spots were corrected. Proteins of interest were extracted and analyzed by using matrix-assisted laser desorption/ionization time-of-flight (MALDI/ToF) MS. In-gel trypsin digestion was performed with a ProGest Protein Digester (Genomic Solutions, Ltd., London, United Kingdom). After preincubation, the digestions were carried out at 37°C for 3 h, using 50 ng sequencing-grade porcine trypsin (5 μl/well; Promega, Southampton, United Kingdom). The digests were analyzed with an Ultraflex MALDI-ToF/ToF mass spectrometer (Bruker Daltonics, Ltd., Coventry, United Kingdom). A 200 Hz nitrogen laser was used to desorb/ionize the matrix/analyte material, and ions were detected in positive ion reflectron mode. Peptide masses obtained from the MALDI-ToF analysis were searched against the Mass Spectrometry Data Base using the Mascot peptide mass-fingerprint program (Matrix Science, Ltd., London, United Kingdom). The results gave a probability-based

Mowse score of $-10 * \log(P)$, where P is the probability that the observed match is a random event. Under those parameters, protein scores <63 were considered statistically significant ($P < 0.05$).

Transcriptomics and proteomics analysis

Raw gene expression data were analyzed with GeneSpring GX 11 (Agilent Technologies). Raw data were normalized with a quantile algorithm, and the baseline was transformed to the median of all samples. Those probes with a flag value of present or marginal in ≥80% of any of the experimental categories were selected for further analysis. The R package RankProd (Bioconductor; *http://bioconductor.org/*) was used to identify differentially expressed genes. Genes were defined as differentially expressed if the percentage of false positives in 1000 permutations of the Rank Products test was <5% and the change in expression was >1.2× in either direction. Genes meeting these criteria were used to generate functional networks and pathway analyses with Ingenuity Pathways Analysis (IPA; Ingenuity Systems, Redwood City, CA, USA). Spearman's correlation tests were performed on the gene sets with a cutoff of 1.2-fold changes in either direction using SPSS Statistics, version 22.0 software (IBM, Armonk, NY, USA). IPA was used to generate functional networks and pathways for the gene sets for which expression correlated significantly with plasma Se status, and the proteomics dataset and the Comparison function in IPA were used to integrate the transcriptomic and proteomic datasets.

RESULTS

Se status of the participants

Participants were selected on the basis of their plasma Se status and divided into 2 groups that were discordant in plasma Se status, but matched for body mass index (24.7 ± 0.88 and 24.1 ± 0.72 in suboptimal and optimal Se groups, respectively), age (53.6 ± 2.91 and 54.7 ± 3.6, in suboptimal and optimal Se groups, respectively), and sex (5 males, 6 females in each group). The Third National Health and Nutrition Examination Survey estimated that the mean serum Se level in the U.S. population is 1.58 μM (16), a level considered to represent Se adequacy (17). In contrast, average plasma Se concentration in healthy British adults was estimated at 1.13 μM (18). The latter concentration is similar to those in other European countries and is considered suboptimal (5). In the present study, the group of participants with plasma Se concentrations similar to that in the U.S. population, having a mean ± SEM plasma Se status concentration of 1.43 ± 0.06 μM (range, 1.25–1.82), a value within the optimal range based on the hazard ratio for mortality (18) was designated as the optimal Se status group. This concentration is well below the Se concentrations (>2.22 μM) that have been associated with adverse health outcomes of high Se doses observed in supplementation trials (4, 17, 19). The suboptimal Se status group corresponds to individuals with a mean ± SEM plasma Se status concentration of 0.86 ± 0.01 μM (range, 0.79–0.92), a range that is suboptimal as defined by the hazard mortality ratio and that has been associated with increased risk of CRC in women in a large European population in the EPIC study (5).

Effects of Se status on gene expression profiles

Both RNA and proteins were extracted from individual rectal biopsies. After microarray analysis, differential gene expression analysis was determined using the RankProd package and a cutoff of 1.2-fold change showed that 254 genes were differentially expressed between the 2 Se groups, with 128 genes being up-regulated and 126 down-regulated in the suboptimal Se group compared with the optimal Se group (for details see *Transcript Profiling*; *http://www.ncbi.nlm.nih.gov/geo/query/acc.cgi?token=epkzqgighfujhkh&acc=GSE70550*).

Two selenoprotein genes (*SEPW1* and *SELK*) were down-regulated in the suboptimal Se group, but they were not among the top 25 down-regulated genes. **Table 1** presents the top 25 genes up- and down-regulated in rectal tissue from the suboptimal Se group compared with the optimal Se group. In the suboptimal Se group, water channel *AQP8*, serine protease inhibitor *SPINK4*, antiapoptotic factor *OLFM4*, chloride channel *CLCA4*, carbonic anhydrase *CA4*, and carcinoembryonic antigens *CEACAM6* and *-7* exhibited the greatest up-regulation. Similarly, other family members (*AQP11*, *SPINK5*, and *CEACAM1* and *-5*) were also upregulated in the suboptimal Se group. In contrast, *HLA-A29.1*, *IL1B*, the transcription factor *CHURC1*, antiapoptotic factors *PHDLA1* and *IER3*, tumor suppressor *ERRFI1/Mig6*, and microRNA *MIR-221* showed the strongest down-regulation in the suboptimal Se group compared with the optimal Se group. Real-time PCR confirmed the microarray results, with significant correlation observed between microarray and real-time-PCR expression for *MFF* ($P = 0.005$) and *ERRFI1* ($P = 0.033$) (data not shown).

Ingenuity Pathway Analysis (IPA) was performed on the microarray dataset to identify biologic functions, canonical pathways, and networks modulated by Se status and to predict potential upstream regulators. A large proportion of genes differentially expressed between the 2 Se groups belonged to cancer [204/254 genes (80%)], gastrointestinal diseases (58%), and inflammatory diseases (39%) categories (**Tables 2 and 3**).

The cell and molecular functions most affected by Se status included cellular growth and proliferation, cellular movement and development, cell death and survival, and cell-to-cell signaling and interaction (Table 2). The 5 most significantly affected canonical pathways corresponded to pathways involved in inflammatory and immune signaling, suggesting an overall down-regulation of immune response in individuals with suboptimal Se status. IPA generated 25 networks, among which 19 had at least 10 focus molecules (data not shown), with the 5 most significantly affected networks presented in Table 3. As a result of these changes, IPA predicted that *PDGFBB* ($P = 2.46E^{-36}$, regulating 114 genes/254), *TNFa* ($P = 3.58E^{-30}$, regulating 145 genes/254), and *IL1b* ($P = 3.31E^{-25}$, regulating 128 genes/254) are likely to be the most important upstream regulators affected by Se status (**Table 4**). In addition, most of the identified upstream regulators (23 of the top 25) are key to immune and inflammatory responses, and the observed changes indicate that this response is inhibited by lower Se status. Crosstalk

TABLE 1. *List of the top 25 genes down-regulated and up-regulated in individuals with suboptimal Se status*

Symbol	Entrez gene name	Fold change	Network	Location	Type	Biomarker application
Top 25 genes down-regulated in suboptimal Se group						
HLA-A29.1	Major histocompatibility complex, class I, A	−2.708	18	Plasma membrane	Other	Efficacy, response to therapy
IL1B	Interleukin 1, β	−1.891	1	Extracellular space	Cytokine	Diagnosis, efficacy, prognosis
CHURC1	Churchill domain containing 1	−1.85	14	Nucleus	Transcription regulator	
PHLDA1	Pleckstrin homology-like domain, family A, member 1	−1.76	3,11	Cytoplasm	Other	
mir-221	microRNA 221	−1.738	2,15	Cytoplasm	mRNA	Unspecified application
ERRFI1	ERBB receptor feedback inhibitor 1	−1.728	3	Cytoplasm	Other	
C11orf96	Chromosome 11 open reading frame 96	−1.666	13	Other	Other	
IER3	Immediate early response 3	−1.647	7,9,16	Cytoplasm	Other	Unspecified application
CCL2	Chemokine (C-C motif) ligand 2	−1.612	5	Extracellular space	Cytokine	Diagnosis, efficacy, prognosis, response to therapy, safety, unspecified application
GSTA1	Glutathione *S*-transferase α 1	−1.557	1	Cytoplasm	Enzyme	
UGT2B17	UDP glucuronosyltransferase 2 family, polypeptide B17	−1.547	8	Cytoplasm	Enzyme	
CSRNP1	Cysteine-serine-rich nuclear protein 1	−1.537	1	Nucleus	Transcription regulator	
TNFRSF12A	Tumor necrosis factor receptor superfamily, member 12A	−1.537	5	Plasma membrane	Transmembrane receptor	
CXCL8	Chemokine (C-X-C motif) ligand 8	−1.528	5	Extracellular space	Cytokine	Diagnosis, efficacy, prognosis, unspecified application
ACKR3	Atypical chemokine receptor 3	−1.502	7	Plasma membrane	G-protein coupled receptor	
EGR1	Early growth response 1	−1.497	14	Nucleus	Transcription regulator	Diagnosis
TPT1	Tumor protein, translationally controlled 1	−1.49	5,19	Cytoplasm	Other	
SERTAD1	SERTA domain containing 1	−1.486	13	Nucleus	Transcription regulator	Unspecified application
RPL8	Ribosomal protein L8	−1.485	19	Other	Other	
PLAU	Plasminogen activator, urokinase	−1.477	3	Extracellular space	Peptidase	Disease progression, efficacy, prognosis
C8orf4	Chromosome 8 open reading frame 4	−1.476	16	Other	Other	
PFKFB3	6-Phosphofructo-2-kinase/fructose-2,6-biphosphatase 3	−1.474	2	Cytoplasm	Kinase	
CCL19	Chemokine (C-C motif) ligand 19	−1.47	10	Extracellular space	Cytokine	Disease progression, unspecified application
NCOA7	Nuclear receptor coactivator 7	−1.466	15	Nucleus	Transcription regulator	
ARL14	ADP-ribosylation factor-like 14	−1.464		Other	Other	
Top 25 genes up-regulated in suboptimal Se group						
AQP8	Aquaporin 8	2.961	17	Plasma membrane	Transporter	
SPINK4	Serine peptidase inhibitor, Kazal type 4	2.303	18	Extracellular space	Other	
OLFM4	Olfactomedin 4	2.071	1	Extracellular space	Other	

(*continued on next page*)

TABLE 1. (*continued*)

Symbol	Entrez gene name	Fold change	Network	Location	Type	Biomarker application
CLCA4	Chloride channel accessory 4	1.962		Plasma membrane	Ion channel	
CA4	Carbonic anhydrase IV	1.71	14	Plasma membrane	Enzyme	
MFF	Mitochondrial fission factor	1.586		Cytoplasm	Other	
CEACAM7	Carcinoembryonic antigen-related cell adhesion molecule 7	1.56	17	Plasma membrane	Other	Diagnosis
GUCA2A	Guanylate cyclase activator 2A (guanylin)	1.554		Extracellular space	Other	
TUBAL3	Tubulin, α-like 3	1.533		Other	Enzyme	
HLA-DRB1	Major histocompatibility complex, class II, DR β 1	1.53	5	Plasma membrane	Transmembrane receptor	
DHRS9	Dehydrogenase/reductase (SDR family) member 9	1.507	3	Cytoplasm	Enzyme	
CEACAM6	Carcinoembryonic antigen-related cell adhesion molecule 6 (non-specific cross reacting antigen)	1.495	2	Plasma membrane	Other	Diagnosis, prognosis
GUCA2B	Guanylate cyclase activator 2B (uroguanylin)	1.442		Extracellular space	Other	
KRT20	Keratin 20, type I	1.439	17	Cytoplasm	Other	Diagnosis, disease progression, prognosis, unspecified application
OAS1	2'-5'-Oligoadenylate synthetase 1, 40/46kDa	1.438	10,17	Cytoplasm	Enzyme	
CEACAM5	Carcinoembryonic antigen-related cell adhesion molecule 5	1.428	2	Plasma membrane	Other	
PLA2G2A	Phospholipase A2, group IIA (platelets, synovial fluid)	1.425	1	Cytoplasm	Enzyme	Efficacy, prognosis, safety
PRR15L	Proline rich 15-like	1.421	4	Other	Other	
AKR1B10	—	1.414	3	Other	Other	
BMP4	Bone morphogenetic protein 4	1.411	6	Extracellular space	Growth factor	
TMIGD1	Transmembrane and immunoglobulin domain containing 1	1.402	17	Other	Other	
LYZ	Lysozyme	1.398	1	Extracellular space	Enzyme	Unspecified application
PSG3	Pregnancy specific β-1-glycoprotein 3	1.382	16	Extracellular space	Other	
RPS23	Ribosomal protein S23	1.374	4	Cytoplasm	Translation regulator	
MUC2	Mucin 2, oligomeric mucus/gel-forming	1.374	11,19	Other	Other	Diagnosis

RNA was isolated from rectal biopsies and subjected to microarray analysis. Genes showing the largest down- or up-regulation were identified by RankProd. The top 25 genes up- or down-regulated are presented, with the corresponding gene symbol and fold change, the networks they belong to as identified by IPA software, the subcellular localization, the type of molecule, and the evidence of biomarker application.

TABLE 2. *Pathway analysis of the microarray and proteomic datasets*

Microarray			Proteomic		
Pathway	*P* range	Molecules(n)	Pathway	*P* range	Molecules(n)
Top biological functions					
Diseases and disorders					
Cancer	5.48E-05–1.00E-34	204	*Cancer*	4.49E-10–1.64E-02	21
Neurological disease	5.23E-05–3.21E-28	105	*Inflammatory response*	2.09E-08–1.54E-02	13
Gastrointestinal disease	3.84E-05–3.63E-23	147	Immunologic disease	7.74E-08 to1.48E-02	14
Inflammatory disease	6.03E-05–2.83E-21	98	Dermatological diseases and conditions	2.14E-07–1.62E-02	17
Organismal injury and abnormalities	4.64E-05–1.16E-20	177	Connective tissue disorders	1.50E-06 to1.48E-02	10
Molecular and cellular functions					
Cellular growth and proliferation	5.99E-05–2.55E-27	179	*Cell death and survival*	1.94E-07–1.35E-02	15
Cellular movement	5.88E-05–3.33E-26	127	*Cellular movement*	7.94E-07–1.62E-02	13
Cellular development	5.99E-05–1.87E-20	155	*Cellular development*	5.31E-06–1.58E-02	13
Cell death and survival	5.38E-05–7.42E-20	151	*Cellular growth and proliferation*	5.31E-06–1.43E-02	15
Cell-to-cell signaling and interaction	3.26E-05–3.44E-11	81	Molecular transport	1.07E-05–1.49E-02	11
Physiological system development and functions					
Immune cell trafficking	5.88E-05–1.10E-19	80	Embryonic development	5.31E-06–1.21E-02	10
Hematological system development and function	5.88E-05–2.98E-17	114	Organismal development	5.31E-06–1.21E-02	13
Tissue morphology	5.88E-05–8.33E-17	86	*Tissue morphology*	5.31E-06–1.62E-02	12
Skeletal and muscular system development and function	5.47E-05–6.67E-16	49	*Hematological System Development and Function*	1.63E-05–1.58E-02	13
Tissue development	4.60E-05–6.67E-16	121	*Immune cell trafficking*	1.63E-05–1.54E-02	7
Top canonical pathways					
Agranulocyte adhesion and diapedesis	2.96E-10	20/189	Inhibition of LXR/RXR activation pathway	2.03E-05	4/121
Granulocyte adhesion and diapedesis	1.68E-07	16/177	Inhibition of FXR/RXR activation pathway	2.46E-05	4/127
Atherosclerosis signaling	4.06E-07	13/123	Acute phase response signaling	7.50E-05	4/169
Hepatic fibrosis/hepatic stellate cell activation	7.19E-07	16/197	Extrinsic prothrombin activation pathway	2.10E-04	2/16
Crosstalk between dendritic cells and natural killer cells	5.14E-06	10/89	Intrinsic prothrombin activation pathway	7.03E-04	2/29

IPA was used to identify biologic functions, canonical pathways, and networks in which mRNAs and proteins are differentially expressed between the suboptimal and optimal Se groups. The 5 most significantly enriched molecular and cellular functions, physiological system functions, and canonical pathways are indicated, together with the corresponding *P* value and number of molecules (n) involved in the datasets. Functions and pathways affected in both datasets are indicated in italics and indented under the 5 most affected canonical pathways belonging to the immune function category.

TABLE 3. *Most significantly affected networks for the microarray and proteomics datasets*

Microarray			Proteomics		
Network	*Z* score	Focus molecules	Network	*Z* score	Focus molecules
Antimicrobial response, *inflammatory response, cellular movement*	35	26	*Inflammatory response, cell death and survival*, connective tissue disorders	38	16
Respiratory system development and function, carbohydrate metabolism, cancer	35	26	*Cellular development, cell death and survival*, cell cycle	18	9
Cellular growth and proliferation, *hematologic system development and function*, tissue morphology	33	25	Molecular transport, carbohydrate metabolism, developmental disorder	3	1
Cancer, organismal injury and abnormalities, reproductive system disease	33	25			
Cellular development, cellular growth and proliferation, *cell death and survival*	31	24			

The most significantly enriched networks are indicated with the *z* score and number of focus molecules. Networks affected in both microarray and proteomics datasets are indicated in italics.

between NFκB, TNFα, PDGFBB, and IL1B signaling pathways (Fig. 3) and between NFκB and other transcription factors, such as p53 and STAT3 (Table 4), has been described (20). Overall, these results indicate that genes involved in immune and inflammatory responses, cell signaling, cell proliferation, tissue and cell morphology, and cellular movement are differentially expressed in response to Se status.

Correlation of gene expression with Se status

RankProd identified genes that exhibit the highest change in expression between the 2 Se groups, but did not define the degree to which gene expression correlated with Se status. Thus, to further investigate the relationship between Se status and gene expression, Spearman's correlation analyses were performed on expression data from

TABLE 4. *Predicted upstream regulators*

Upstream regulator	Molecule type	Predicted activation state	Activation *z* score	*P* of overlap	Target molecules in dataset (*n*)
PDGF BB	Complex	Inhibited	−4.672	2.46E-36	114
TNF	Cytokine	Inhibited	−2.883	3.58E-30	145
IL1B	Cytokine	Inhibited	−2.584	3.31E-25	128
SP1	Transcription regulator		−0.808	4.40E-20	101
TREM1	Transmembrane receptor	Inhibited	−2.593	6.32E-19	128
IL6	Cytokine	Inhibited	−2.161	7.33E-18	128
IFNG	Cytokine		−0.682	8.83E-18	121
NFκB (complex)	Complex	Inhibited	−2.275	1.64E-17	143
TGFB1	Growth factor		−1.782	2.88E-17	146
CREB1	Transcription regulator	Inhibited	−2.584	2.25E-16	81
α-Catenin	Group		0.895	2.71E-16	49
STAT3	Transcription regulator	Inhibited	−2.979	5.98E-16	119
IRAK4	Kinase		−1.135	9.12E-16	114
IgG	Complex		1.833	9.78E-16	126
IL1A	Cytokine	Inhibited	−2.535	1.30E-15	88
PI3K (complex)	Complex		0.299	2.43E-15	132
Jnk	Group	Inhibited	−2.736	3.55E-15	135
P38 MAPK	Group		−1.211	8.03E-15	146
TLR3	Transmembrane receptor		−1.318	1.22E-14	129
Cg	Complex	Inhibited	−3.384	2.18E-14	124
TP53	Transcription regulator		−1.432	3.38E-14	149
ERK	Group	Inhibited	−2.113	9.28E-14	120
CEBPA	Transcription regulator		0.613	1.43E-13	101
RET	Kinase	Inhibited	−2.970	7.22E-13	89
FAS	Transmembrane receptor		1.328	8.18E-13	132

IPA upstream transcriptional regulator analysis was performed to identify the cascade of potential upstream regulators that can explain the observed gene expression changes in the microarray dataset. The most likely regulators are presented, together with the type of molecule, the number of known targets for each upstream regulator present in the dataset, the predicted *z* score activation state, the *P* value of overlap between genes targeted by each regulator in the dataset, and the genes known to be a target for each upstream regulator.

all participants for the 254 genes modulated by Se status, using plasma Se concentration as a continuous variable. Expression of 69 genes (recognized by 75 different gene probes) correlated significantly with Se status, of which 34 correlated positively and 35 correlated negatively (Supplemental Table S1 and **Fig. 1**). Expression of the 2 selenoprotein genes *SELW* and *SELK*, identified as being down-regulated in the suboptimal Se group, showed a strong positive correlation with Se status ($\rho_{Selw} = 0.637$; $P = 0.001$, and $\rho_{Selk} = 0.474$; $P = 0.026$). Expression of *DNAJC12*, a member of the DnaJ/Hsp40 family acting as a cochaperone with Hsp70 and involved in protein folding and export (21); antisense RNA *SNHG6*; and *SEPW1* showed the strongest positive correlations with Se concentration. Hsp70 is involved in nonsense-mediated decay (22) and has been involved in the control of selenoprotein mRNA degradation in conditions of low Se status (23). In contrast, expression of acyl-coenzyme A oxidase *ACOX1*, the first enzyme in peroxisomal fatty acid β-oxidation, strongly negatively correlated with Se status. Because *ACOX1* activates NFκB (24), negative correlation of *ACOX1* expression with Se status could contribute to the observed NFκB inhibition. Moreover, *NUAK2*, which is regulated by NFκB and is involved in actin cytoskeleton remodelling (25), and *ACTB*, *ALDOA*, *SLC9A3R1*, *MYH9*, *DYNLRB1*, and *TUBAL3*, which are implicated in cytoskeleton organization (26, 27), had expression that correlated strongly with Se status.

Subsequently, pathway analysis of the 69 genes for which expression correlated strongly with Se status revealed that the most affected diseases and disorders correspond to the cancer and cancer and tumorigenesis subcategories (34 molecules/69; 49%; $P = 1.71E^{-05}$–$4.93E^{-02}$) and to inflammatory response (18 molecules/69; 26%; $P = 4.88E^{-05}$–$4.67E^{-02}$). Three main networks identified were: *1*) cancer, organismal injury, and abnormalities, reproductive system disease (21 focus molecules, *z* score 45), centered around NFκB; *2*) cellular function and maintenance carbohydrate metabolism, small-molecule biochemistry (16 focus molecules, *z* score 31), centered around TNF; and *3*) hematologic disease, cellular growth and proliferation, cellular development (9 focus molecules, *z* score 15) centered around TP53 (Supplemental Fig. S1). Supporting these observations, inhibition of sequestosome 1 (*SQSTM1*), which regulates TNF-driven activation of NFκB, was identified as the most significant upstream regulator ($P = 2.50E^{-06}$), followed by *PLK2* and *IL13*, also involved in NFκB regulation, the second and third most significant ($P = 4.09E^{-05}$ and $P = 4.61E^{-05}$, respectively). Overall, these results indicate that genes whose expression correlate with Se status play a key role in inflammatory pathways, with a central role for NFκB and TNF.

Effects of Se status on proteomics profiles

Proteomic profiles from whole rectal biopsies were characterized by 2-D gel electrophoresis, followed by in-gel trypsin digestion and MALDI-ToF MS. To limit the bias normally associated with proteomic analysis when the analysis is restricted toward the more abundant proteins, analysis was performed on all 220 spots that were identified by MS. Of these 220, 36 spots, corresponding to 26 individual proteins, were differentially expressed between the suboptimal Se and optimal Se status groups (**Table 5**). They include a substantial proportion [13/36 spots; 7/26 (~ 26%) proteins] of cytoskeleton proteins: *1*) 4 cytokeratins and desmin, *2*) actin ACTA2, and *3*) tubulin TUBA1B. In addition, 4 proteins known to be involved in the

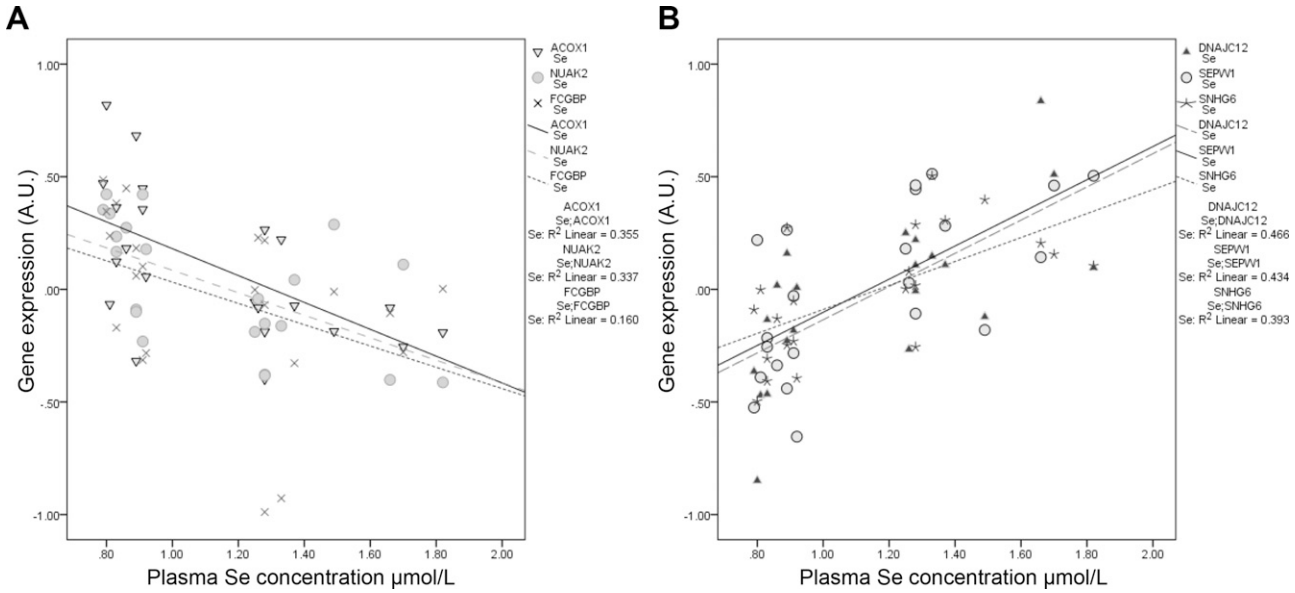

Figure 1. Correlation of gene expression with plasma Se concentration. Spearman's correlation was performed on the gene set generated by microarray analysis, to identify expression of genes that significantly correlate with plasma Se concentration. Scatterplots show the relationship between gene expression and Se status for genes with the strongest negative (*A*) or positive (*B*) correlation coefficient. A list of genes with expression significantly correlated with Se status is presented in Supplemental Table S1.

cytoskeletal organization, SS18, S100A9, SFN, and HSP90B, exhibited differential expression between the 2 Se groups. These observations suggest that cytoskeleton remodelling is a major signature of Se effects in rectal tissue. All cytoskeletal proteins and associated factors were up-regulated in the suboptimal Se group compared with the optimal Se group, apart from 1 spot corresponding to cytokeratin 8 and S100A9.

Additional proteins differentially expressed between the 2 Se groups (Table 5) include: *1*) proteins involved in immune and inflammatory response (tumor rejection antigen GP96 (HSP90B1), complement component C3, glycyl-tRNA synthetase (28) and calcium-binding protein S100A9); *2*) proteins involved in lipid metabolism and disruption of cholesterol homeostasis known to be linked to inflammatory processes (29) and to affect signal transduction and membrane trafficking (29) (FABP5, apolipoprotein A1, StAR-related lipid transfer protein); and *3*) proteins involved in antioxidant mechanisms, including glutathione *S*-transferase ω 1 (GSTO1), S100A9, and albumin. The lowered expression of these genes in the

TABLE 5. *Proteins differentially expressed in suboptimal and optimal Se groups*

Symbol	Entrez gene name	UniProt/ Swiss-Prot accession	Fold change	*P*	Network	Location	Type
Optimal Se group							
HBB	Hemoglobin, β	P68871	2.287862	1.57E-02	1	Cytoplasm	Transporter
KRT9	Keratin 9	P35527	2.136131	3.99E-02		Other	Other
TUBA1B	Tubulin, α 1b	B3KPS3	1.649467	7.15E-03	2	Cytoplasm	Other
HSP90B1	Heat shock protein 90 kDa β (Grp94), member 1	P14625	1.60214	1.94E-02	1,2	Cytoplasm	Other
LAP3	Leucine aminopeptidase 3	P28838	1.566994	1.66E-02	2	Cytoplasm	Peptidase
KRT19	Keratin 19	P08727	1.561573	1.17E-03	1	Cytoplasm	Other
SS18	Synovial sarcoma translocation, chromosome 18	Q15532	1.536875	1.20E-02	2	Nucleus	Transcription regulator
STARD4	Star-related lipid transfer (START) domain containing 4	Q96DR4	1.461044	2.55E-02	1	Cytoplasm	Transporter
KRT10	Keratin 10	P13645	1.417157	2.15E-03	1	Cytoplasm	Other
ACTA2	Actin, α 2, smooth muscle, aorta	P62736	1.355664	4.27E-02	1	Cytoplasm	Other
SFN	Stratifin	P31947	1.250929	4.12E-02	2	Cytoplasm	Other
DES	Desmin	P17661	1.249196	4.81E-02	1	Cytoplasm	Other
FABP5	Fatty acid binding protein 5 (psoriasis-associated)	Q01469	1.164734	4.86E-02	1	Cytoplasm	Transporter
Suboptimal Se group							
GALE	UDP-galactose-4-epimerase	Q14376	0.853818	4.49E-02	3	Cytoplasm	Enzyme
SERPINC1	Serpin peptidase inhibitor, clade C (antithrombin), member 1	P01008	0.789494	1.09E-02	1	Extracellular space	Enzyme
GARS	Glycyl-tRNA synthetase	P41250	0.783497	4.30E-02	2	Cytoplasm	Enzyme
A2ML1	α-2–Macroglobulin-like 1	A8K2U0	0.782412	3.50E-02		Cytoplasm	Other
HPX	Hemopexin	P02790	0.757333	2.35E-02	1	Extracellular space	Transporter
S100A9	S100 calcium binding protein A9	P06702	0.747425	1.00E-02	1	Cytoplasm	Other
APOA1	Apolipoprotein A-I	P02647	0.746389	3.93E-02	1	Extracellular space	Transporter
G6PD	Glucose-6-phosphate dehydrogenase	P11413	0.716481	5.06E-03	1	Cytoplasm	Enzyme
ALB	Albumin	P02768	0.712025	3.30E-02	1, 2	Extracellular space	Transporter
GSTO1	Glutathione *S*-transferase ω 1	P78417	0.68968	7.87E-03	2	Cytoplasm	Enzyme
KRT8	Keratin 8	P05787	0.625898	2.22E-02	1	Cytoplasm	Other
C3	complement component 3	B4E216	0.622869	1.59E-02	1	Extracellular space	Peptidase
F13A1	coagulation factor XIII, A1 polypeptide	P00488	0.59791	1.97E-02	2	Extracellular space	Enzyme

After, 2-D gel electrophoresis, proteins were identified by MALDI/ToF MS. Differentially expressed proteins between the 2 Se groups are presented, together with their UniProt (*http://www.uniprot.org*) identification (ID), and the *P* value and fold change estimated from 2-D gel quantification.

suboptimal Se group not only suggests a reduced immunity and capacity to protect against oxidative damage, but is compatible with the links between glutathione and Se metabolism. Moreover, the cytoskeleton, a key mediator of immune and inflammatory processes (30, 31), is highly sensitive to oxidative stress (32).

IPA analysis of the proteomic data also predicted activation of cancer pathways (z score activation, 2.575; $P = 2.89E^{-09}$; focus molecules, 21) in individuals with suboptimal Se status. Consistent with observations from RNA expression analysis by microarray, immunologic and inflammatory responses biologic functions and networks, together with cell death and survival, cellular movement and development, cell growth and differentiation, and hematologic system and molecular transport (Table 2) were among the most affected by Se status. IPA identified 3 networks, with network 1, centered around NFκB (focus molecules, 16; z score 38), representing the most important one (Table 3).

Integrated transcriptomics and proteomics

Tables 2 and 3 summarize the pathways and networks altered by Se status in transcriptomic and proteomic datasets. To integrate the 2 approaches, the datasets were combined, and IPA was used to identify biologic processes or pathways in which features from both transcripts and proteins are enriched. Twenty-eight networks were identified, and the interconnection between proteomic and transcriptomic networks was analyzed. Proteomic network 1 is connected to 8 networks from the microarray dataset, and proteomic network 2 is connected to 6 microarray networks. Merging proteomic network 1 (p 1) with individual connected microarray networks (4–7 and 10 m) revealed NFκB to be the central node of these merged networks (**Fig. 2**) and IL1, TNF, and Akt to be the central nodes of merged networks 1-1, 1-18, and 1-12, respectively (data not shown). On the other hand, the proto-oncogenes c-*Myc*, c-*Fos* and β-catenin were identified as central nodes from merging proteomic network 2, with connected microarray networks 2 and 8, 4, and 6 (data not shown).

DISCUSSION

This study is the first to integrate transcriptomic and proteomic approaches for assessing the effects of physiologic differences in status of the dietary antioxidant Se on events in the large-bowel mucosa in healthy individuals. Using this approach, we report that the expression of factors implicated in inflammatory signaling, immune function, and cytoskeleton remodelling is altered in individuals with suboptimal Se status in healthy human rectal mucosa,

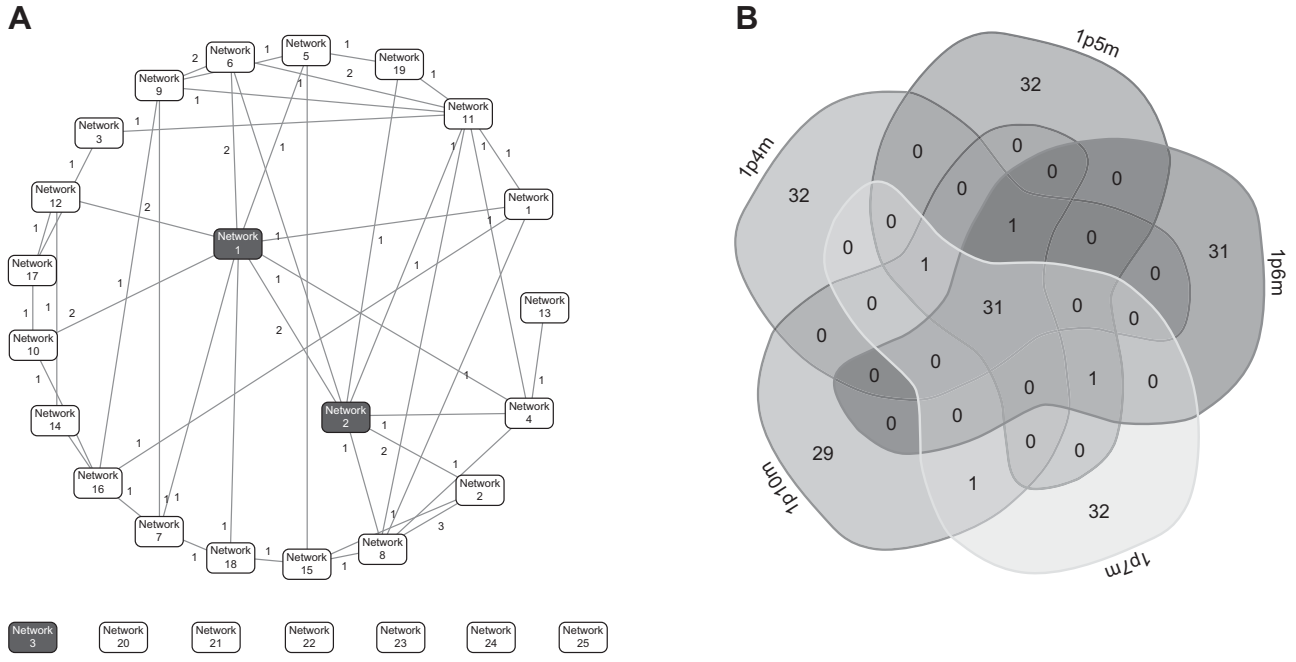

Figure 2. Interconnection between networks identified from proteomic and transcriptomic datasets. *A*) IPA analysis performed on the combined proteomic and transcriptomic datasets revealed 28 networks, corresponding to 25 microarray networks (white background) and 3 proteomic networks (dark gray background). Connections between these networks are represented by lines. Figures adjacent to the lines indicate the number of common genes shared between pathways. Major proteomic networks 1 and 2 are interconnected and showed connections with 8 and 6 microarray networks, respectively. This information was used to identify central regulatory nodes for interconnected networks. *B*) With this approach, NFκB was identified as a common central node for 5 of 8 merged networks involving proteomic network 1 (1 p) and microarray network (4–7 and 10 m). The Venn diagram presents the number of molecules shared by these merged networks.

providing novel insights into the mechanisms through which Se may influence cancer risk and colorectal function. Crosstalk between these pathways is fundamental to the maintenance of gut homeostasis through a partnership among the gut epithelium, immune cells, and responses to bacteria (33). Among the genes and proteins exhibiting the strongest change in expression between the 2 Se groups (Tables 1 and 5), many have been shown to have altered expression in colorectal adenomas.

As expected differences in selenoprotein mRNA expression were observed between the 2 groups, with significant reduction of both selenoprotein W [fold change (FC) = −1.404] and selenoprotein K (FC = −1.286) in the suboptimal group (Gene Expression Omnibus repository, GSE70550; *http://www.ncbi.nlm.nih.gov/geo/*). Moreover, expression of both *SEPW1* and *SELK* correlated strongly with Se status (Supplemental Table S1), consistent with the responsiveness of selenoproteins to Se in the colon. It is known that identification of selenoproteins using MS is problematic, and it is therefore not surprising that our proteomic analysis did not identify specific selenoproteins.

We observed significant effects of Se status on immune and inflammatory signaling in both the microarray and proteomics datasets (Table 2), with approximately a third of identified genes (80/254) and proteins (7/26) involved in immune cell trafficking, with most canonical pathways associated with inflammation, and with inflammatory and immune diseases and inflammatory

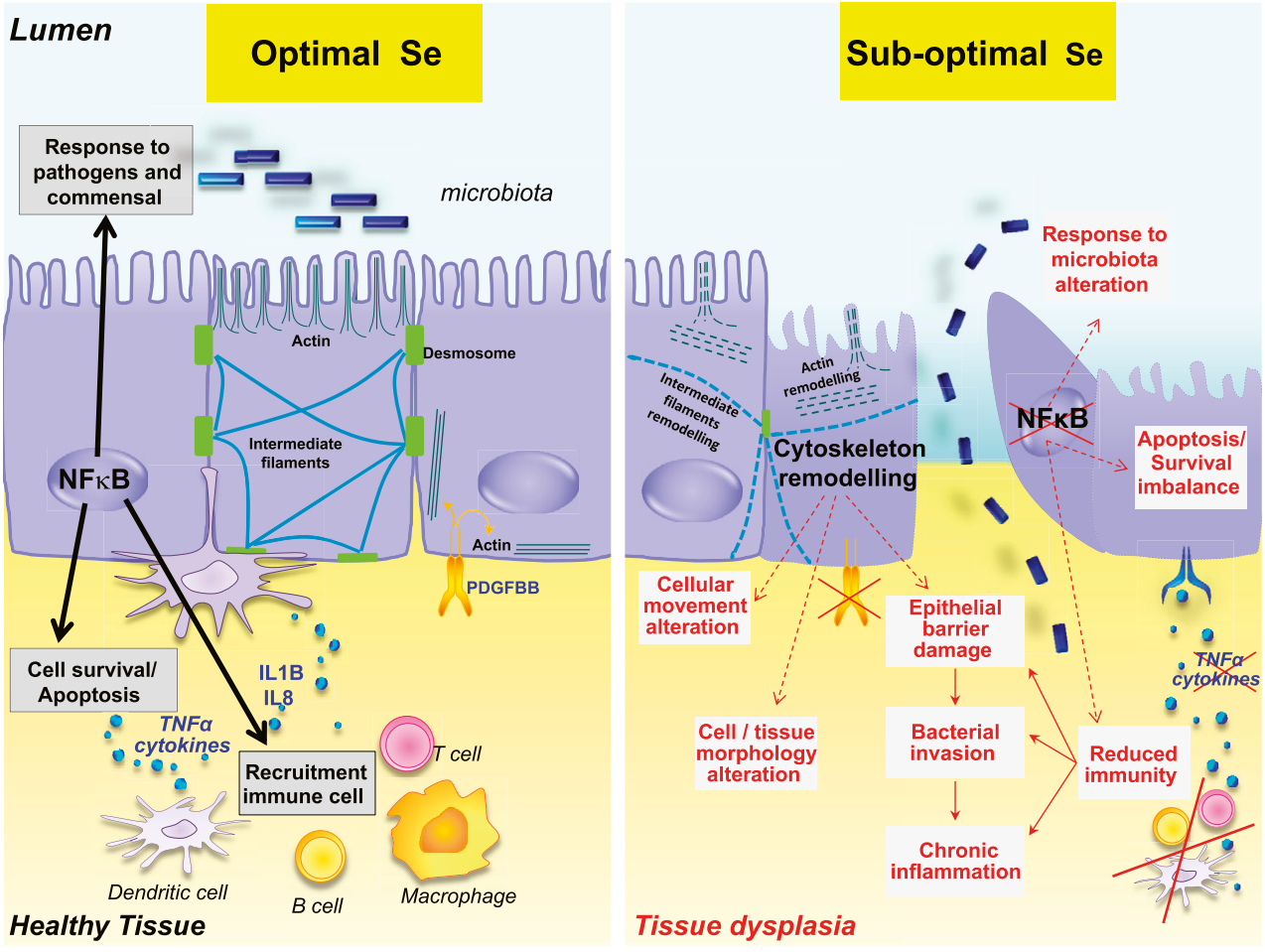

Figure 3. Hypothetical model illustrating the integration of observed effects of suboptimal Se status on colorectal function. This model illustrates how the observed changes in gene expression and protein levels affect inflammatory and immune signaling, cytoskeletal remodelling and apoptotic/survival pathways, and how these changes and crosstalk between these pathways have the potential to contribute to tissue dysplasia in the rectum of an individual with suboptimal Se status. In the healthy colorectal epithelium, NFκB plays a critical role of coordinator, regulating: *1*) cytokine and chemokine production (blue circle) in response to the gut bacteria (blue rectangles), *2*) the recruitment of immune cells (red, yellow, and beige) to the epithelium to ensure immuno-surveillance, and *3*) the regulation of the balance between survival and apoptotic factors. We propose that NFκB inhibition, as a result of suboptimal Se status, reduces immune and inflammatory signaling and induces cytoskeleton remodelling (changes associated with suboptimal Se are indicated in red and dotted lines). Cytoskeletal alteration and imbalance of apoptotic/survival signals could result in epithelial barrier damage and changes in cell and tissue morphology and cell movement. Moreover, the combined alteration of the epithelial barrier, reduced expression of IL1B and IL8, and reduced immunity could favor bacterial invasion, leading to chronic inflammation.

response among the top biologic functions and networks in both datasets. Genes exhibiting the largest fold changes in expression included those involved in the immune response (*HLA-A29.1* and *HLA-DRB1)*, growth factors and cytokines (*BMP4*, *CCL19*, *CCL12*, *IL1B*, and *IL8*), genes previously reported to be associated with either inflamed colonic epithelium [*OLFM4* (34) and *SPINK4* (35, 36)] or colorectal cancer [*AQP8* and *OLFM4* (37, 38)], and tumor suppressor genes [*ERRFI1* and *PHLDA1* (39)] (Table 1). Furthermore, a large number of proteins identified by proteomics are key players in inflammation and immune function (*e.g.*, ApoA1, Serpin C1, S1009, C3, HPX, HSP90B1, and G6PD). Integrating the 2 datasets identified NFκB, IL1, TNF, and Akt, which play key roles in inflammation, as central nodes of merged networks (Fig. 2*B*). Moreover, most of the highly significant predicted upstream regulators were cytokines and growth factors involved in inflammation and immune response (Table 4). Pathway analysis of genes for which expression correlated significantly with Se status highlighted the central regulatory role of NFκB and TNFα. *SELK* expression, which correlated positively with Se status (Supplemental Table S1), has been identified recently as a key player in the immune response and in calcium signaling pathways (40, 41). Thus, overall pathway and network analysis was consistent with both a reduction of inflammatory signaling capacity and inhibition of NFκB and proinflammatory cytokines TNFα and IL1B in rectal tissue of individuals with suboptimal Se status. Because NFκB plays a central role in coordinating the response to gut microflora and the inflammatory signaling response, we propose that inadequate Se status results in disruption of the coordination by NFκB of immune and inflammatory responses with the potential to contribute to the transformation process (**Fig. 3**). This theory is supported by previous observations that NFκB signaling and inflammatory response pathways were altered in the colon of mice fed a diet marginally deficient in Se (13, 42), and inhibition of NFκB signaling in epithelial cells leads to spontaneous development of severe inflammatory conditions in mice (43). Dysregulation of immune and inflammatory functions are central to colorectal carcinogenesis (20).

Proteomic data indicated that relatively small differences in Se status were associated with changes in abundance of a substantial proportion of cytoskeletal proteins, including cytokeratins, desmin, actin, and tubulin (Table 5). Cytokeratins have key regulatory functions, and actin microfilaments maintain the integrity of the epithelial barrier and cell polarity (44). Consequently, cellular movement, growth and proliferation and tissue morphology were among the most affected biologic functions identified by IPA (Table 2). Consistent with these observations, the same biologic functions were affected significantly at the mRNA level (Table 2). This finding suggests the potential for substantial remodelling of the cytoskeleton in rectal mucosa in response to suboptimal Se status. This process would be expected to a have major impact on the colonic epithelium as it undergoes normal cycles of proliferation, migration, and differentiation. Indeed, previous work has found altered expression of cytoskeletal components in CRC; desmoglein 2 and cytokeratins KRT18, KRT6A, and KRT8 were identified as signatures of CRC subtypes (45), high expression of desmin was associated with CRC and cytokeratins 8, 10, 18, and 19 and β-actin were up-regulated in CRC tumors (46). In addition, previous work has indicated a role for the cytoskeleton in mediating the immune and inflammatory responses (30, 31).

In the present study, both RNA and proteins were extracted from rectal biopsy tissues, which are complex with multiple cell types and at different stages of differentiation. Therefore the results reflect changes in protein and RNA profiling from diverse cell types of both epithelial and immune origin, and changes in the proportions of these 2 major cell types may account for some of the observed effects. However, we have no reason to believe that there are any systematic differences in cellularity of the biopsies between those with normal and suboptimal Se status, and this complexity takes into account the different cellular actors present in the rectal mucosa.

Overall, the present data indicate that, in the macroscopically normal rectal mucosa, suboptimal Se status is associated with alterations in cytoskeleton remodelling and reduced inflammatory and immune signaling capacity. This finding suggests that the inflammatory response and the capacity to recruit immune cells are reduced in the rectum of individuals with suboptimal Se status. Colorectal cancer is characterized by derangements in immune and inflammatory signaling and cytoskeleton alterations. We hypothesize that suboptimal Se status has the potential to compromise an individual's redox capacity and ability to mount appropriate immune and inflammatory responses to exogenous, physiologic, or microbiological stressors and, as a result, could favor the development of cancer (Fig. 3). In support of this hypothesis, cancer pathways were identified as the most affected pathways in both proteomic and transcriptomic datasets. Recent evidence from genetic association studies has led to the hypothesis of a convergence of hormones, inflammation, and energy-related factors (CHIEF) pathway in the etiology of CRC (29). We propose that the convergence of reduced immunity and inflammatory response and cytoskeleton remodelling associated with reduced Se status would increase CRC risk. FJ

C.M. was supported by the Newcastle Healthcare Charity and the Biotechnology and Biological Sciences Research Council (BBSRC) (BB/H011471/1). I.T.J., A.C.J.P., and F.M. were supported by a contract from the United Kingdom Food Standards Agency (N12015) and by a BBSRC strategic grant to the Institute of Food Research. A.Z. was supported by funds from Grant BB/H011471/1 from the Biotechnology and Biological Sciences Research Council (awarded to J.E.H. and J.C.M.). The authors declare no conflicts of interest.

REFERENCES

1. Jacobs, E. T., Jiang, R., Alberts, D. S., Greenberg, E. R., Gunter, E. W., Karagas, M. R., Lanza, E., Ratnasinghe, L., Reid, M. E., Schatzkin, A., Smith-Warner, S. A., Wallace, K., and Martínez, M. E. (2004) Selenium and colorectal adenoma: results of a pooled analysis. *J. Natl. Cancer Inst.* **96**, 1669–1675
2. Nutritional Prevention of Cancer Study Group. (1996) Effects of selenium supplementation for cancer prevention in patients with carcinoma of the skin. A randomized controlled trial. *JAMA* **276**, 1957–1963
3. Takata, Y., Kristal, A. R., King, I. B., Song, X., Diamond, A. M., Foster, C. B., Hutter, C. M., Hsu, L., Duggan, D. J., Langer, R. D., Petrovitch, H., Shikany, J. M., Vaughan, T. L., Lampe, J. W., Prentice, R. L., and Peters, U. (2011) Serum selenium, genetic variation in selenoenzymes, and risk of colorectal cancer: primary analysis from the Women's Health Initiative Observational Study and meta-analysis. *Cancer Epidemiol. Biomarkers Prev.* **20**, 1822–1830
4. Lippman, S. M., Klein, E. A., Goodman, P. J., Lucia, M. S., Thompson, I. M., Ford, L. G., Parnes, H. L., Minasian, L. M., Gaziano, J. M., Hartline, J. A., Parsons, J. K., Bearden III, J. D., Crawford, E. D., Goodman, G. E., Claudio, J., Winquist, E., Cook, E. D., Karp, D. D., Walther, P., Lieber, M. M., Kristal, A. R., Darke, A. K., Arnold, K. B., Ganz, P. A., Santella, R. M., Albanes, D., Taylor, P. R., Probstfield, J. L., Jagpal, T. J., Crowley, J. J., Meyskens, F. L., Jr., Baker, L. H., and Coltman, C. A., Jr. (2009) Effect of selenium and vitamin E on risk of prostate cancer and other cancers: the Selenium and Vitamin E Cancer Prevention Trial (SELECT). *JAMA* **301**, 39–51
5. Hughes, D. J., Fedirko, V., Jenab, M., Schomburg, L., Méplan, C., Freisling, H., Bueno-de-Mesquita, H. B., Hybsier, S., Becker, N. P., Czuban, M., Tjønneland, A., Outzen, M., Boutron-Ruault, M. C., Racine, A., Bastide, N., Kühn, T., Kaaks, R., Trichopoulos, D., Trichopoulou, A., Lagiou, P., Panico, S., Peeters, P. H., Weiderpass, E., Skeie, G., Dagrun, E., Chirlaque, M. D., Sánchez, M. J., Ardanaz, E., Ljuslinder, I., Wennberg, M., Bradbury, K. E., Vineis, P., Naccarati, A., Palli, D., Boeing, H., Overvad, K., Dorronsoro, M., Jakszyn, P., Cross, A. J., Quirós, J. R., Stepien, M., Kong, S. Y., Duarte-Salles, T., Riboli, E., and Hesketh, J. E. (2015) Selenium status is associated with colorectal cancer risk in the European prospective investigation of cancer and nutrition cohort. *Int. J. Cancer* **136**, 1149–1161
6. Reddy, B. S., Rivenson, A., El-Bayoumy, K., Upadhyaya, P., Pittman, B., and Rao, C. V. (1997) Chemoprevention of colon cancer by organoselenium compounds and impact of high- or low-fat diets. *J. Natl. Cancer Inst.* **89**, 506–512
7. Finley, J. W., and Davis, C. D. (2001) Selenium (Se) from high-selenium broccoli is utilized differently than selenite, selenate and selenomethionine, but is more effective in inhibiting colon carcinogenesis. *Biofactors* **14**, 191–196
8. Peters, U., Chatterjee, N., Hayes, R. B., Schoen, R. E., Wang, Y., Chanock, S. J., and Foster, C. B. (2008) Variation in the selenoenzyme genes and risk of advanced distal colorectal adenoma. *Cancer Epidemiol. Biomarkers Prev.* **17**, 1144–1154
9. Méplan, C., and Hesketh, J. (2012) The influence of selenium and selenoprotein gene variants on colorectal cancer risk. *Mutagenesis* **27**, 177–186
10. Bellinger, F. P., Raman, A. V., Reeves, M. A., and Berry, M. J. (2009) Regulation and function of selenoproteins in human disease. *Biochem. J.* **422**, 11–22
11. Cole-Ezea, P., Swan, D., Shanley, D., and Hesketh, J. (2012) Glutathione peroxidase 4 has a major role in protecting mitochondria from oxidative damage and maintaining oxidative phosphorylation complexes in gut epithelial cells. *Free Radic. Biol. Med.* **53**, 488–497
12. Gong, G., Méplan, C., Gautrey, H., Hall, J., and Hesketh, J. E. (2012) Differential effects of selenium and knock-down of glutathione peroxidases on TNFα and flagellin inflammatory responses in gut epithelial cells. *Genes Nutr.* **7**, 167–178
13. Kipp, A., Banning, A., van Schothorst, E. M., Méplan, C., Schomburg, L., Evelo, C., Coort, S., Gaj, S., Keijer, J., Hesketh, J., and Brigelius-Flohé, R. (2009) Four selenoproteins, protein biosynthesis, and Wnt signalling are particularly sensitive to limited selenium intake in mouse colon. *Mol. Nutr. Food Res.* **53**, 1561–1572
14. Tapp, H. S., Commane, D. M., Bradburn, D. M., Arasaradnam, R., Mathers, J. C., Johnson, I. T., and Belshaw, N. J. (2013) Nutritional factors and gender influence age-related DNA methylation in the human rectal mucosa. *Aging Cell* **12**, 148–155
15. Polley, A. C., Mulholland, F., Pin, C., Williams, E. A., Bradburn, D. M., Mills, S. J., Mathers, J. C., and Johnson, I. T. (2006) Proteomic analysis reveals field-wide changes in protein expression in the morphologically normal mucosa of patients with colorectal neoplasia. *Cancer Res.* **66**, 6553–6562
16. Niskar, A. S., Paschal, D. C., Kieszak, S. M., Flegal, K. M., Bowman, B., Gunter, E. W., Pirkle, J. L., Rubin, C., Sampson, E. J., and McGeehin, M. (2003) Serum selenium levels in the US population: Third National Health and Nutrition Examination Survey, 1988-1994. *Biol. Trace Elem. Res.* **91**, 1–10
17. Rayman, M. P. (2012) Selenium and human health. *Lancet* **379**, 1256–1268
18. Sunde, R. A., Paterson, E., Evenson, J. K., Barnes, K. M., Lovegrove, J. A., and Gordon, M. H. (2008) Longitudinal selenium status in healthy British adults: assessment using biochemical and molecular biomarkers. *Br. J. Nutr.* **99**(Suppl 3), S37–S47
19. Laclaustra, M., Stranges, S., Navas-Acien, A., Ordovas, J. M., and Guallar, E. (2010) Serum selenium and serum lipids in US adults: National Health and Nutrition Examination Survey (NHANES) 2003–2004. *Atherosclerosis* **210**, 643–648
20. Hoesel, B., and Schmid, J. A. (2013) The complexity of NF-κB signaling in inflammation and cancer. *Mol. Cancer* **12**, 86
21. Lee, J., Hahn, Y., Yun, J. H., Mita, K., and Chung, J. H. (2000) Characterization of JDP genes, an evolutionarily conserved J domain-only protein family, from human and moths. *Biochim. Biophys. Acta* **1491**, 355–363
22. Popp, M. W., and Maquat, L. E. (2013) Organizing principles of mammalian nonsense-mediated mRNA decay. *Annu. Rev. Genet.* **47**, 139–165
23. Zemolin, A. P., Meinerz, D. F., de Paula, M. T., Mariano, D. O., Rocha, J. B., Pereira, A. B., Posser, T., and Franco, J. L. (2012) Evidences for a role of glutathione peroxidase 4 (GPx4) in methylmercury induced neurotoxicity in vivo. *Toxicology* **302**, 60–67
24. Li, Y., Tharappel, J. C., Cooper, S., Glenn, M., Glauert, H. P., and Spear, B. T. (2000) Expression of the hydrogen peroxide-generating enzyme fatty acyl CoA oxidase activates NF-kappaB. *DNA Cell Biol.* **19**, 113–120
25. Legembre, P., Schickel, R., Barnhart, B. C., and Peter, M. E. (2004) Identification of SNF1/AMP kinase-related kinase as an NF-kappaB-regulated anti-apoptotic kinase involved in CD95-induced motility and invasiveness. *J. Biol. Chem.* **279**, 46742–46747
26. Jin, Q., Liu, G., Domeier, P. P., Ding, W., and Mulder, K. M. (2013) Decreased tumor progression and invasion by a novel anti-cell motility target for human colorectal carcinoma cells. *PLoS One* **8**, e66439
27. Takubo, T., Wakui, S., Daigo, K., Kurokata, K., Ohashi, T., Katayama, K., and Hino, M. (2003) Expression of non-muscle type myosin heavy polypeptide 9 (MYH9) in mammalian cells. *Eur. J. Histochem.* **47**, 345–352
28. Park, M. C., Kang, T., Jin, D., Han, J. M., Kim, S. B., Park, Y. J., Cho, K., Park, Y. W., Guo, M., He, W., Yang, X. L., Schimmel, P., and Kim, S. (2012) Secreted human glycyl-tRNA synthetase implicated in defense against ERK-activated tumorigenesis. *Proc. Natl. Acad. Sci. USA* **109**, E640–E647
29. Slattery, M. L., and Fitzpatrick, F. A. (2009) Convergence of hormones, inflammation, and energy-related factors: a novel pathway of cancer etiology. *Cancer Prev. Res. (Phila.)* **2**, 922–930
30. Rogers, K. R., Morris, C. J., and Blake, D. R. (1992) The cytoskeleton and its importance as a mediator of inflammation. *Ann. Rheum. Dis.* **51**, 565–571
31. Vicente-Manzanares, M., and Sánchez-Madrid, F. (2004) Role of the cytoskeleton during leukocyte responses. *Nat. Rev. Immunol.* **4**, 110–122
32. Banan, A., Choudhary, S., Zhang, Y., Fields, J. Z., and Keshavarzian, A. (1999) Ethanol-induced barrier dysfunction and its prevention by growth factors in human intestinal monolayers: evidence for oxidative and cytoskeletal mechanisms. *J. Pharmacol. Exp. Ther.* **291**, 1075–1085
33. Clark, J. A., and Coopersmith, C. M. (2007) Intestinal crosstalk: a new paradigm for understanding the gut as the "motor" of critical illness. *Shock* **28**, 384–393
34. Shinozaki, S., Nakamura, T., Iimura, M., Kato, Y., Iizuka, B., Kobayashi, M., and Hayashi, N. (2001) Upregulation of Reg 1alpha

and GW112 in the epithelium of inflamed colonic mucosa. *Gut* **48**, 623–629
35. Häsler, R., Feng, Z., Bäckdahl, L., Spehlmann, M. E., Franke, A., Teschendorff, A., Rakyan, V. K., Down, T. A., Wilson, G. A., Feber, A., Beck, S., Schreiber, S., and Rosenstiel, P. (2012) A functional methylome map of ulcerative colitis. *Genome Res.* **22**, 2130–2137
36. Wapenaar, M. C., Monsuur, A. J., Poell, J., van 't Slot, R., Meijer, J. W., Meijer, G. A., Mulder, C. J., Mearin, M. L., and Wijmenga, C. (2007) The SPINK gene family and celiac disease susceptibility. *Immunogenetics* **59**, 349–357
37. Moon, C., Soria, J. C., Jang, S. J., Lee, J., Obaidul Hoque, M., Sibony, M., Trink, B., Chang, Y. S., Sidransky, D., and Mao, L. (2003) Involvement of aquaporins in colorectal carcinogenesis. *Oncogene* **22**, 6699–6703
38. Besson, D., Pavageau, A. H., Valo, I., Bourreau, A., Belanger, A., Eymerit-Morin, C., Mouliere, A., Chassevent, A., Boisdron-Celle, M., Morel, A., Solassol, J., Campone, M., Gamelin, E., Barre, B., Coqueret, O., and Guette, C. (2011) A quantitative proteomic approach of the different stages of colorectal cancer establishes OLFM4 as a new nonmetastatic tumor marker. *Mol. Cell Proteomics* **10**, M111.009712
39. Sakthianandeswaren, A., Christie, M., D'Andreti, C., Tsui, C., Jorissen, R. N., Li, S., Fleming, N. I., Gibbs, P., Lipton, L., Malaterre, J., Ramsay, R. G., Phesse, T. J., Ernst, M., Jeffery, R. E., Poulsom, R., Leedham, S. J., Segditsas, S., Tomlinson, I. P., Bernhard, O. K., Simpson, R. J., Walker, F., Faux, M. C., Church, N., Catimel, B., Flanagan, D. J., Vincan, E., and Sieber, O. M. (2011) PHLDA1 expression marks the putative epithelial stem cells and contributes to intestinal tumorigenesis. *Cancer Res.* **71**, 3709–3719
40. Verma, S., Hoffmann, F. W., Kumar, M., Huang, Z., Roe, K., Nguyen-Wu, E., Hashimoto, A. S., and Hoffmann, P. R. (2011) Selenoprotein K knockout mice exhibit deficient calcium flux in immune cells and impaired immune responses. *J. Immunol.* **186**, 2127–2137
41. Meiler, S., Baumer, Y., Huang, Z., Hoffmann, F. W., Fredericks, G. J., Rose, A. H., Norton, R. L., Hoffmann, P. R., and Boisvert, W. A. (2013) Selenoprotein K is required for palmitoylation of CD36 in macrophages: implications in foam cell formation and atherogenesis. *J. Leukoc. Biol.* **93**, 771–780
42. Kipp, A. P., Banning, A., van Schothorst, E. M., Meplan, C., Coort, S. L., Evelo, C. T., Keijer, J., Hesketh, J., and Brigelius-Flohe, R. (2012) Marginal selenium deficiency down-regulates inflammation-related genes in splenic leukocytes of the mouse. *J. Nutr. Biochem.* 23, 1170–1177
43. Pasparakis, M. (2009) Regulation of tissue homeostasis by NF-kappaB signalling: implications for inflammatory diseases. *Nat. Rev. Immunol.* **9**, 778–788
44. Stein, M., Wandinger-Ness, A., and Roitbak, T. (2002) Altered trafficking and epithelial cell polarity in disease. *Trends Cell Biol.* **12**, 374–381
45. NCI CPTAC. (2014) Proteogenomic characterization of human colon and rectal cancer. *Nature* **513**, 382–387
46. Alfonso, P., Núñez, A., Madoz-Gurpide, J., Lombardia, L., Sánchez, L., and Casal, J. I. (2005) Proteomic expression analysis of colorectal cancer by two-dimensional differential gel electrophoresis. *Proteomics* **5**, 2602–2611

Received for publication February 8, 2016.
Accepted for publication April 12, 2016.